HAYATI
Journal of Biosciences

Vol. 32 No. 5, September 2025 1260-1272
DOI:10.4308/hjb.32.5.1260-1272
ISSN: 1978-3019
EISSN: 2086-4094

Research Article

Integrated DNA Barcoding and Morphometric Characterization of Palm Weevils (*Rhynchophorus* spp.) in North Sulawesi

Endrile Golmen Balansa[1], Christina Leta Salaki[1], Dantje Tarore[1], Juliet Merry Eva Mamahit[1], Beivy Jonathan Kolondam[1,2], Trina Ekawati Tallei[2*]

[1]*Doctoral Program in Entomology, Graduate Program, Sam Ratulangi University, Manado 95115, Indonesia*
[2]*Department of Biology, Faculty of Mathematics and Natural Sciences, Sam Ratulangi University, Manado 95115, Indonesia*

ARTICLE INFO

Article history:
Received April 13, 2025
Received in revised form May 7, 2025
Accepted June 2, 2025

KEYWORDS:
DNA barcoding,
phylogenetic analysis,
genetic distance,
morphometric variation,
pest identification,
barcode gap

ABSTRACT

Palm weevils (*Rhynchophorus* spp.) are significant pests of sago palms worldwide. Yet, the taxonomy and evolutionary lineage of these species in North Sulawesi remain unclear, likely due to geographic isolation driving genetic variation and species differentiation. This study aimed to investigate the genetic diversity and morphological differentiation of *Rhynchophorus across* distinct geographic regions in North Sulawesi using an integrative approach combining DNA barcoding and morphometric analysis. Morphometric traits from palm weevil specimens collected in Sangihe Island, Minahasa, and Bolaang Mongondow were measured and statistically analyzed using one-way ANOVA, MANOVA, principal component analysis (PCA), and linear discriminant analysis (LDA) to assess interpopulation morphological differences. For molecular identification, the cytochrome oxidase I (COI) gene was amplified and sequenced. Phylogenetic relationships were inferred using the maximum likelihood method, and a DNA barcode gap analysis was conducted to evaluate the separation between intra- and interspecific genetic distances. Morphometric analysis revealed significant size variations among the specimens, particularly in rostrum dimensions, with the EBBM (Bolaang Mongondow) group showing the highest values. COI-gene-based identification confirmed that all specimens were of *R. vulneratus*. However, phylogenetic analysis showed EBMin (Minahasa) and EBBM forming a distinct subgroup, while EBMan, EBSTS, EBTam, and EBSTU (all from Sangihe Island) clustered separately. Barcode gap analysis demonstrated a clear distinction between intra- and interspecific divergence, validating COI as a reliable marker for species delimitation. This study concludes that integrating morphometric and genetic analyses reveals geographic structuring within *R. vulneratus*, highlighting the effectiveness of combined methods for accurate identification and population differentiation.

1. Introduction

Rhynchophorus spp., commonly known as palm weevils, are insects that frequently damage various palm species (Seman-Kamarulzaman *et al.* 2023). These weevils are globally distributed across Asia, Africa, the Americas, and Europe (Rochat *et al.* 2017). In Southeast Asia, three species have been identified as major pests: *R. ferrugineus* (red palm weevil), *R. vulneratus* (Asiatic palm weevil), and *R. bilineatus* (black palm weevil). In Indonesia, *R. vulneratus* and *R. bilineatus* have been reported as pests of palm trees in several provinces, including Aceh, Java, Yogyakarta, Madura, and North Sulawesi (Sukirno *et al.* 2018). Morphological and physicochemical differences among *Rhynchophorus* spp. infesting *Arenga pinnata* (sugar palm), *Metroxylon sagu* (sago palm), and *Cocos nucifera* (coconut) in Minahasa, North Sulawesi, indicate that *Rhynchophorus* spp. associated with sago and coconut exhibit close genetic

* Corresponding Author
E-mail Address: trina_tallei@unsrat.ac.id

relatedness. In contrast, those from sugar palms form a distinct node, showing greater similarity to *R. vulneratus* (Korua *et al.* 2016).

The sago palm is a widely distributed palm species found across various regions of Indonesia, including Sumatra, Sulawesi, Papua, and Maluku (Ehara *et al.* 2020). This plant thrives in yellow-brown or black clay soils with high organic matter content, as well as in volcanic soils, with an optimal temperature range of 24.5-29°C, a minimum temperature of 15°C, and a relative humidity of 90% (Hastuty 2016). The Sangihe Islands in North Sulawesi are rich in volcanic soil and support extensive sago cultivation, covering 1.6 hectares with a yield of 2,145 tons in 2018 (Direktorat Jenderal Perkebunan Kementerian Pertanian Republik Indonesia 2020). Sago palm plays a crucial role in the survival of *Rhynchophorus* spp., serving as both a natural food source and an oviposition site (Yong *et al.* 2015).

The study of palm weevil in North Sulawesi is essential due to the region's high biodiversity within the Wallacea zone (Stelbrink *et al.* 2012) and the unresolved taxonomy and lineage of these weevils, which are believed to have originated from South Asia and Melanesia (Rugman-Jones *et al.* 2013). Geographic isolation can lead to genetic changes through mutations, as evidenced by previous research documenting morphological differences among species-such as the red-striped, Asiatic, black, and red palm weevils-and variations linked to different host plants, including sago palm, coconut, and oil palm (Nurlydia *et al.* 2019). Environmental pressures may thus drive species variation or the emergence of new species (Edelaar 2018), further supported by the invasive nature and high adaptability of *Rhynchophorus* spp. (Montagna *et al.* 2015).

Accurate species identification and lineage determination of palm weevil require phylogenetic reconstruction using reliable and precise parameters (Al-Saqer 2012), as morphological approaches alone are insufficient to detect genetic variations (Stout *et al.* 2024). DNA barcoding using the mitochondrial gene Cytochrome Oxidase I (COI) has proven highly effective across nearly all animal species (Tallei *et al.* 2017; Lombogia *et al.* 2020). Mitochondrial DNA analysis has been extensively applied to study evolution, population structure, gene flow, hybridization, biogeography, and phylogeny (Antonacci *et al.* 2023; Kolondam *et al.* 2023). Other mitochondrial genes, such as cytochrome b (Cyt b), are also commonly used to examine relationships among closely related taxa (Caraballo *et al.* 2021; Alrefaei *et al.* 2023). The COI gene is particularly crucial because it encodes cytochrome oxidase, a protein essential for oxygen reception in the respiratory chain (Ramzan *et al.* 2021). Its highly conserved nucleotide sequence, minimal insertions and deletions, and low variability make it an ideal genetic barcode for species identification and phylogenetic reconstruction at the species level (Sholihah *et al.* 2020).

Although *Rhynchophorus* spp. are recognized as significant pests of palm species, data on their genetic diversity and species differentiation in North Sulawesi remain limited. Previous studies have primarily focused on morphological traits, while the genetic relationships among local populations are still poorly understood. This study addresses this gap by applying COI-based DNA barcoding to assess the genetic diversity and phylogeny of *Rhynchophorus* spp. in the region, along with species delineation using DNA barcode gap analysis to distinguish intra- and interspecific genetic variation.

2. Materials and Methods

2.1. Morphometric Analysis

Adult (imago) female specimens were manually collected from sago palm trunks in the Sangihe Islands of North Sulawesi, specifically at locations in Manganitu (EBMan), Tamako (EBTam), North Tabukan (EBTU), and South Tabukan (EBTS). Additional specimens were also collected from Minahasa (EBBM) and Bolaang Mongondow (EBMin) of North Sulawesi for comparative analysis. The collection sites are shown in Figure 1. The collection took place during June–July 2024. The live imago samples of palm weevil were subsequently transported to the laboratory and preserved in a 70% ethanol solution. Morphometric analyses were then performed using a Hirox KH8700 3D digital stereomicroscope equipped with measurement software. The morphological characters analyzed included rostrum length (RL), rostrum width (RW), scape length (SL), pedicel length (PL), antennal club length (ACL), antennal club width (ACW), distance between eyes (ED), pronotum length (ProL), pronotum width (ProW), elytra length (EL), elytra width (EW), mesocoxal distance (MsC), metacoxal distance (MtC), meso-metacoxal distance (MstD), pygidium length (PyL), and body length (BL). The morphological characterization of *Rhynchophorus* spp. was based on the criteria outlined previously (Rozziansha *et al.* 2021). Measurements were taken using a Carl Zeiss binocular microscope and a Hirox KH8700 3D digital stereomicroscope, and

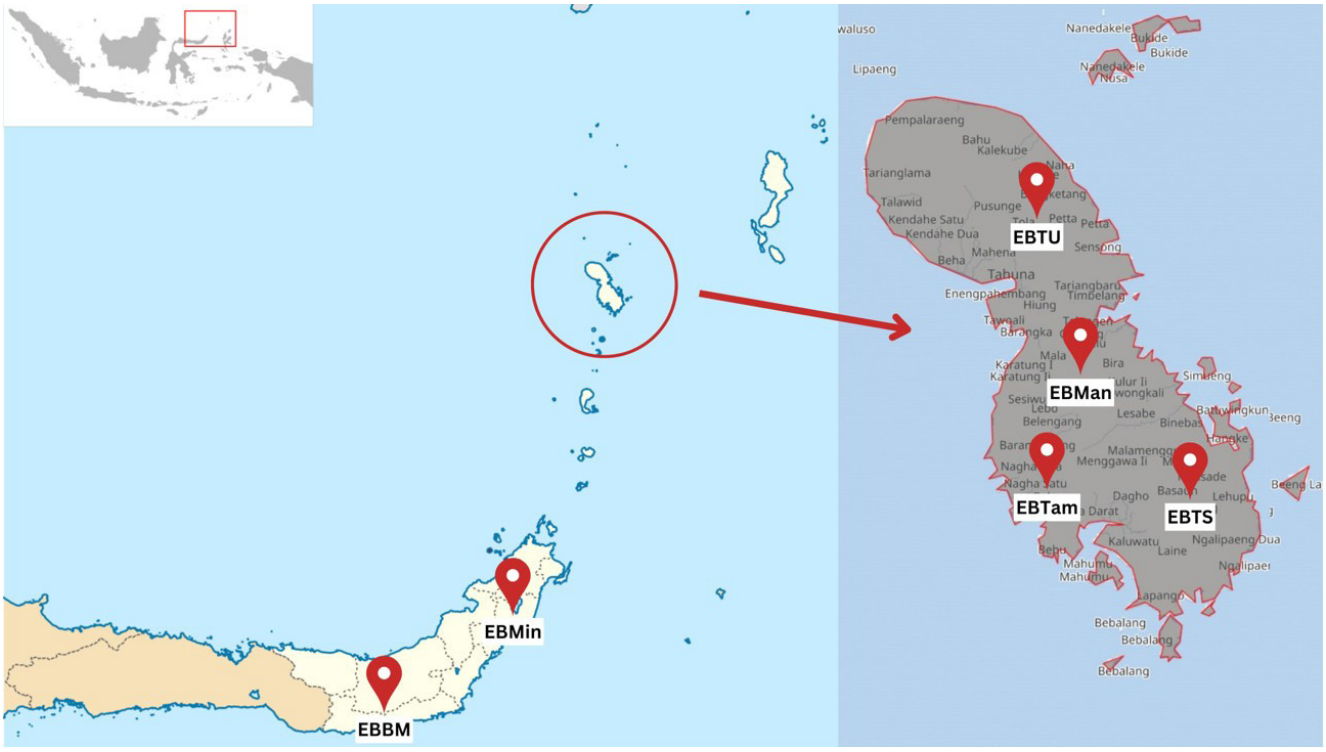

Figure 1. Collection sites of adult (imago) female specimens from sago palm trunks in the Sangihe forests of North Sulawesi (Manganitu [EBMan], Tamako [EBTam], North Tabukan [EBTU], and South Tabukan [EBTS]), with additional specimens obtained from Minahasa (EBBM) and Bolaang Mongondow (EBMin) for comparative analysis

the results were compared with an existing database of *Rhynchophorus* spp. morphological characters.

Statistical analyses were performed using Python (version 3.8, Python Software Foundation, Wilmington, DE) with the following packages: SciPy (version 1.9.0) for analysis of variance (ANOVA), stats models (version 0.13.0) for multivariate analysis of variance (MANOVA), and sci-kit-learn (version 1.2.0) for principal component analysis (PCA) and linear discriminant analysis (LDA). Key statistical assumptions were tested prior to all analyses. Specifically, normality was assessed using the Shapiro-Wilk test for each variable within groups, and homogeneity of variances was evaluated using Levene's test. Q-Q plots and residual plots were examined to verify normality assumptions further. Box's M-test was conducted to assess the homogeneity of covariance matrices for MANOVA. ANOVA was used to assess statistically significant differences among groups ($\alpha = 0.05$). For multivariate analyses, both PCA and LDA were performed after standardizing variables to zero mean and unit variance. Boxplots were generated using seaborn (version 0.12.0) to visualize the distribution, central tendency, and variability of the data, as well as to identify potential outliers. Outliers were defined as observations falling beyond 1.5 times the interquartile range and were individually examined for measurement accuracy.

2.2. DNA Barcoding Analysis

Imago samples of palm weevil were preserved in a 90% ethanol solution before DNA extraction and purification were performed using a tissue genomic DNA Mini Kit (Geneaid) (Tallei *et al.* 2021). The front legs of the specimens were dissected, and the internal tissue was homogenized in 200 µL of GT buffer using a micropestle. The mixture was incubated at 60°C for 30 minutes, followed by the addition of 200 µL GBT buffer and further incubation for 20 minutes. After centrifugation at 10,000 rpm for 1 minute, the supernatant was mixed with cold absolute ethanol and applied to a GC column preassembled with a collection tube. Following centrifugation, the column was washed sequentially with W1 and wash buffers, each followed by centrifugation and discarding of the filtrate. The column was then dried by an additional spin, transferred to a clean tube, and eluted with 150 µL of elution buffer. The purified DNA was stored at 10°C. DNA purity and concentration were assessed using a

nano-spectrophotometer; samples with an A260/A280 ratio of 1.8-2.0 and a concentration of 35 µg/ml were considered suitable for COI gene amplification.

PCR amplification of the COI gene was performed using the primers LCO1490 and HC02198 (Folmer *et al.* 1994; Satiman *et al.* 2022) on a Rotor-Gene Q Real-Time PCR instrument. Each 40 µL reaction contained MyTaq HS Red Mix, primers (10 µM), ddH_2O, and 2 µL of DNA template. The PCR program included initial denaturation at 95°C (3 min), followed by 35 cycles of denaturation (95°C, 20 s), annealing (50°C, 30 s), and extension (72°C, 20 s), with a final extension at 72°C for 1 min. Amplicons were visualized via agarose gel electrophoresis in TBE buffer, and sequencing was conducted to confirm the COI gene sequence.

COI sequences were first compared to reference databases using BLAST (https://blast.ncbi.nlm.nih.gov/Blast.cgi) to identify species. A phylogenetic tree was then built using the maximum likelihood method with 1,000 bootstrap replicates in PhyML v3.3.20180621 (Guindon *et al.* 2010) through Geneious Prime (v2025.1.1) to examine evolutionary relationships. The Kimura 2-parameter (K2P) model (Kimura 1980) was used to calculate genetic distances and evaluate both interspecific and intraspecific variation. This model is widely employed in DNA barcoding due to its ability to distinguish between transition and transversion rates, yielding more reliable estimates of evolutionary divergence (Nishimaki & Sato 2019). A barcode gap analysis was also performed to distinguish clearly between the highest genetic distance observed within species and the lowest distance observed between species (Phillips *et al.* 2024). The presence of a distinct gap between these values will support the effectiveness of COI sequences in accurately delineating species boundaries.

3. Results

3.1. Morphological Variation of Palm Weevil Specimens

Palm weevil specimens were collected from several administrative regions in North Sulawesi to examine morphological variation among populations. Figure 2 shows the specimens obtained directly from the Sangihe Islands, Minahasa, and Bolaang Mongondow Regencies. Table 1 provides a summary of the key morphological measurements of these specimens. Morphometric analysis revealed significant size variations among specimen groups (EBMan, EBTS, EBTU, EBTam, EBBM, and EBMin). In particular, the EBBM specimens exhibited higher morphological measurements, especially in rostrum length (RL) and rostrum width (RW). Boxplot visualizations (Figure 3) consistently showed that EBBM had higher values for these characters, as well as for antennal club length and width, with clear differences in median values and distribution across groups.

The comprehensive morphometric analysis of palm weevil populations from different locations reveals striking differentiation patterns. Assumption checks were conducted prior to all statistical analyses. The Shapiro-Wilk test and Q-Q plots indicated that most morphometric variables were approximately normally distributed within groups, with a few minor deviations. Levene's test indicated heterogeneity of

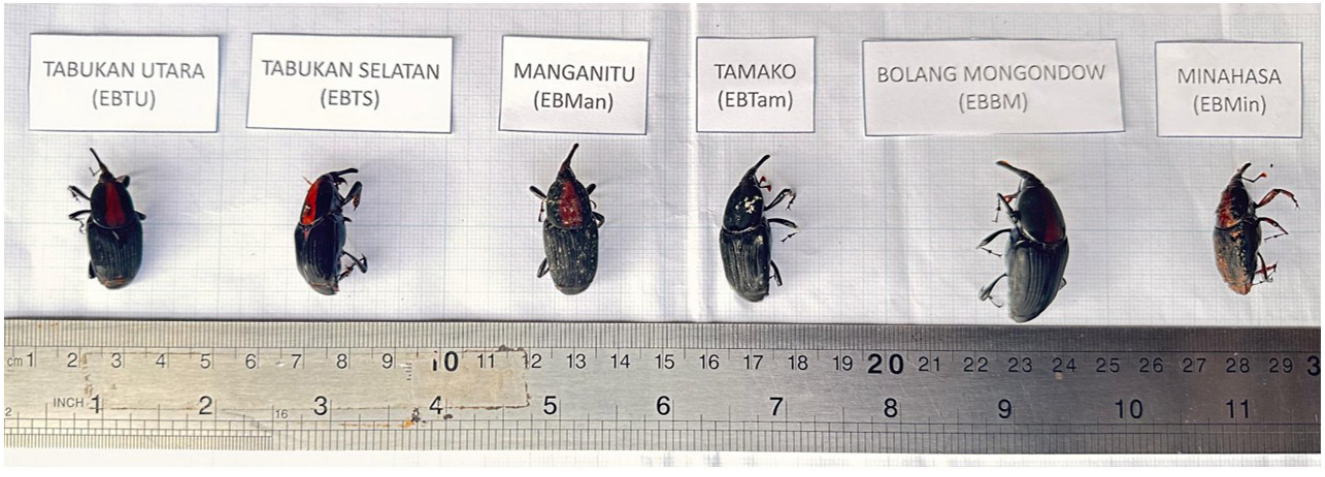

Figure 2. Specimens of palm weevil from Manganitu (EBMan), South Tabukan (EBTS), North Tabukan (EBTU), Tamako (EBTam), EBMin (Minahasa) and Bolaang Mongondow (EBBM)

Table 1. Morphometric measurements of *Rhynchophorus* specimens from Sangihe Talaud, Minahasa, and Bolaang Mongondow are presented in millimeters

Characters	EBMan	EBTS	EBTU	EBTam	EBBM	EBMin
Rostrum length (RL)	12.2±0.40	11.4±0.05	11±0.11	12.2±0.39	19.5±0.43	11.5±0.10
Rostrum width (RW)	4.4±0.29	3.4±0.76	3.3±0.08	4.5±0.77	11.4±0.88	3.4±0.84
Scape length (SL)	6.5±0.18	5.5±0.55	5.4±0.40	6.6±0.10	13.3±.34	5.5±0.57
Pedicel length (PL)	5.5±0.32	4.5±0.87	4.5±0.25	5.4±0.78	12.5±0.07	4.6±0.05
Antennal club length (ACL)	4.3±0.21	3.2±0.95	3.2±0.10	4.3±0.20	11.2±0.96	3.3±0.21
Antennal club width (ACW)	4.6±0.10	3.6±0.70	3.6±0.18	4.6±0.30	11.6±1.02	3.6±0.89
Distance between eyes (ED)	3.8±0.14	2.8±0.25	2.7±0.10	3.8±0.83	10.8±0.55	2.8±0.47
Pronotum length (ProL)	13.7±0.82	12.8±1.10	12.8±0.76	13.6±0.93	20.8±0.38	12.9±0.36
Pronotum width (ProW)	13±0.25	12±0.68	12±0.34	13.1±0.46	20±0.67	12±0.73
Elytra length (EL)	17.5±0.65	16.8±0.15	16.6±0.95	17.5±0.60	24.8±0.22	16.8±0.40
Elytra width (EW)	15±0.31	14.2±0.40	14.1±1.00	15±0.40	22.2±0.28	14.3±0.35
Meso coxal distance (MsC)	5.4±0.35	4.2±0.80	4.2±0.30	5.5±0.12	12.2±0.40	4.3±0.04
Meta coxal distance (MtC)	5.8±0.48	4.8±0.59	4.8±0.31	5.9±0.48	12.8±0.15	4.8±1.05
Meso-meta coxal distance (MstD)	9.8±0.12	8.7±0.10	8.6±0.72	9.8±0.05	16.7±0.34	8.7±0.35
Pygidium length (PyL)	7.7±0.30	6.7±0.72	6.7±0.50	7.8±0.65	14.7±0.30	6.7±1.10

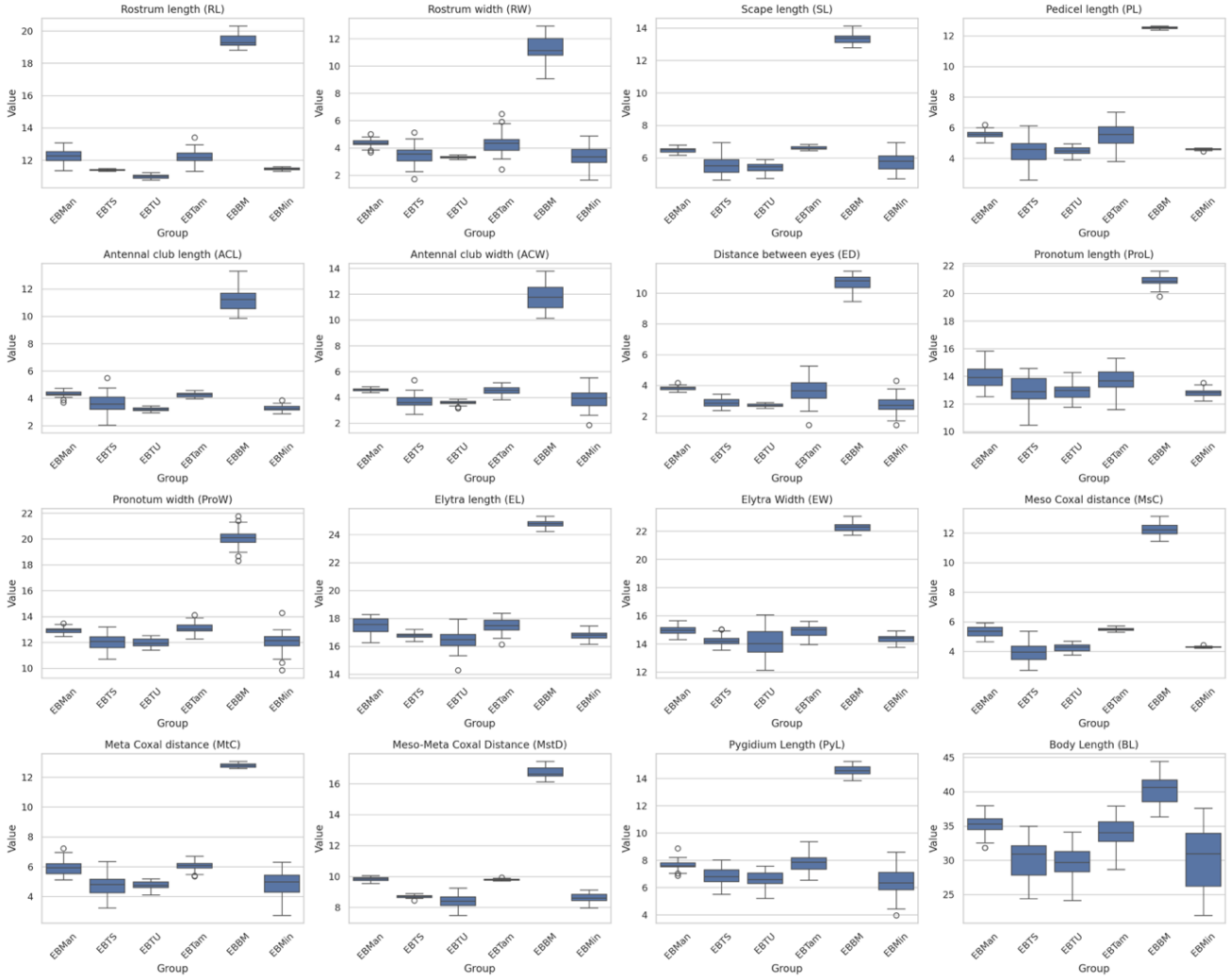

Figure 3. Boxplots illustrating the distribution of morphometric values for various characters (e.g., rostrum length, rostrum width, scape length, etc.) across six specimen groups (EBMan, EBTS, EBTU, EBTam, EBBM, and EBMin). The plots demonstrate significant differences among groups, as confirmed by ANOVA analyses (with very small p-values for all characters), indicating that these morphological variations are statistically robust and not due to random chance

variances across traits. One-way ANOVA across 15 morphometric traits demonstrates highly significant differences between location groups, with all p-values extremely small (ranging from 5.39×10^{-180} to 2.12×10^{-103}). Rostrum length emerged as the most distinct trait ($F = 4272.44$, $p = 5.39 \times 10^{-180}$), followed by scape length ($F = 2131.35$, $p = 4.98 \times 10^{-154}$) and meso-meta coxal distance ($F = 1858.48$, $p = 6.06 \times 10^{-149}$), confirming strong morphometric structuring by geographic location.

Rostrum length (RL) ranged from 11 to 19.5 mm, with EBBM exhibiting the highest value. Similarly, EBBM specimens displayed the greatest rostrum width (RW) at 11.4 mm, while other groups ranged from 3.3 to 4.5 mm. Additional significant differences were observed in scape length (SL), pedicel length (PL), and antennal club length (ACL). Body length (BL) was also highest in EBBM at 40 mm, compared to 30-35 mm in other groups. Other traits, including eye size, pronotum, elytra, and pygidium dimensions, followed similar trends, with larger measurements in EBBM. Measurement consistency was indicated by small standard deviations, except for RW and SL, which showed greater variability. These results suggest that morphological differences likely reflect ecological adaptations or genetic divergence, reinforcing the distinctiveness of each population.

The MANOVA results indicated significant morphometric differences among palm weevil populations, with high Pillai's trace (5.55) and Hotelling-Lawley trace values demonstrating substantial multivariate differences despite a small sample size. PCA and LDA analyses revealed that the first principal component captured over 96% of the variance, with rostrum length (RL), meso-meta coxal distance (MstD), and scape length (SL) emerging as key discriminators among locations. LDA visualization showed a clear separation of populations, suggesting that geographical isolation may drive morphological differentiation.

The three-dimensional (3D) PCA plot (Figure 4) illustrates the distribution of palm weevil samples in principal component space, highlighting the contribution of morphometric variables. PC1 accounts for 96.65% of the variance, while PC2 explains 0.46%, indicating that nearly all morphometric variation is captured by PC1, likely reflecting overall size differences. The plot distinctly separates the EBBM group from other samples, which remain closely clustered. This pattern suggests that EBBM exhibits consistent morphological differences, likely driven by traits such as rostrum or scape length, while the other samples share more similar profiles despite individual variability. The divergence of EBBM may indicate local adaptation or distinct genetic traits. Overall, PCA reveals dominant variance patterns and underscores how certain populations, like EBBM, deviate from more homogenous groups.

LDA of the palm weevil morphometric data revealed distinct clustering patterns among populations from different locations (Figure 5). The EBBM population formed a completely isolated cluster along both the LD1 and LD2 axes, indicating that these weevils possess highly distinctive morphometric traits-possibly due to unique evolutionary adaptations or genetic isolation. In contrast, the EBMan and EBTam populations exhibited partial overlap, suggesting morphometric similarities that may result from gene flow, similar selection pressures, or a shared evolutionary history. The EBTS group formed a relatively distinct cluster with minimal overlap, reflecting moderate morphometric differentiation, while the EBTU and EBMin populations occupied intermediate positions with some overlap, indicating partial similarity. Moreover, the overall arrangement of clusters along the LD1 axis, which captures the most significant discriminating features, suggests a gradient of morphometric variation potentially driven by geographical or ecological factors. These findings confirm that location-based morphometric differences are statistically significant and reinforce the evidence from PCA, highlighting clear, location-specific morphometric signatures in these palm weevil populations.

3.2. COI-Based Genetic Divergence and Species Delimitation

The COI sequence of EBBM exhibited the highest genetic similarity (97.72%) with *R. vulneratus* (accession number MG051025.1), while EBMin showed the closest similarity (98.02%) to *R. vulneratus* (accession number MG051026.1). In contrast, EBMan, EBSTS, EBSTU, and EBTam shared 91.49% sequence similarity with *R. vulneratus* (MG051025.1).

The genetic similarity among North Sulawesi specimens is summarized in Table 2. Pairwise COI sequence analysis reveals that EBBM and EBMin exhibit the highest similarity at 99.24%, reflecting a close genetic relationship, which is consistent with

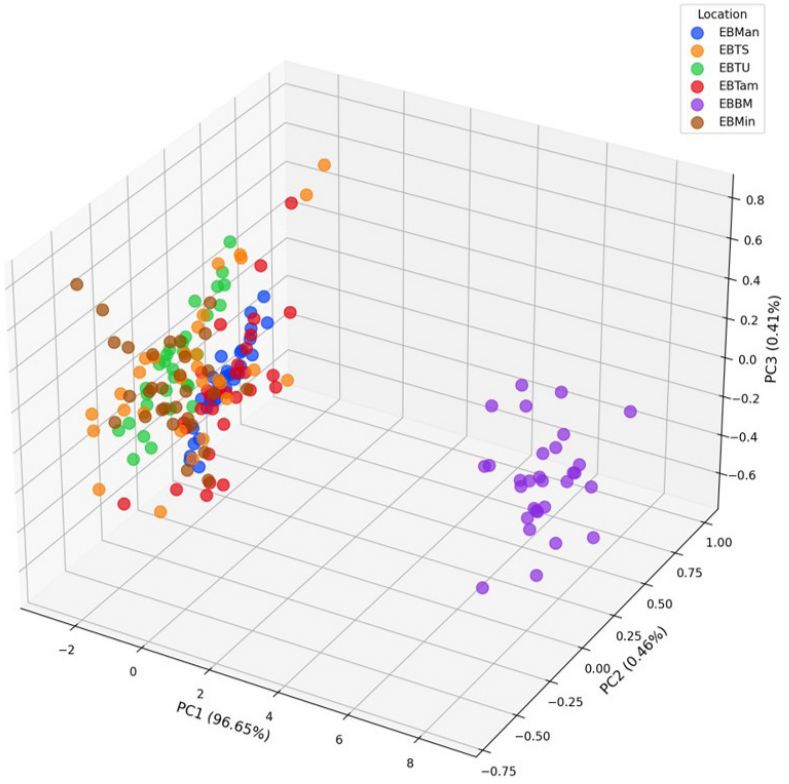

Figure 4. 3D PCA plot of palm weevil morphometric data showing distinct separation of the EBBM group from the relatively clustered other samples. This suggests that key traits-such as rostrum and scape length-drive the primary variation along PC1, highlighting potential local adaptation or unique genetic characteristics in the EBBM population

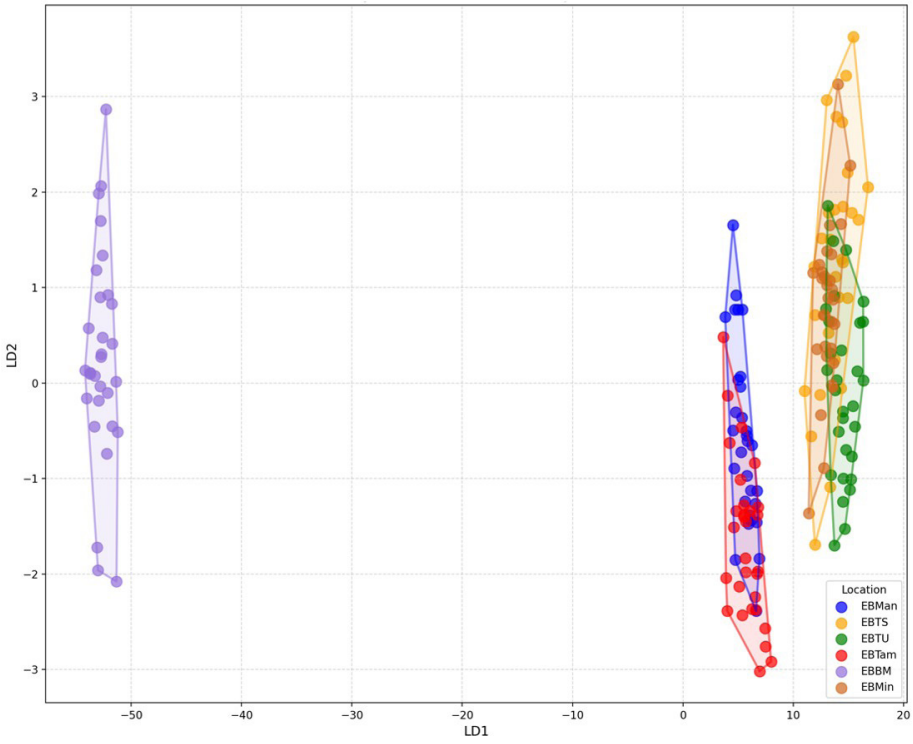

Figure 5. LDA projection of palm weevil morphometric data showing distinct clustering: EBBM (light purple) forms an isolated group, EBMan (blue) and EBTam (red) partially overlap; and EBTS (orange), EBTU (green), and EBMin (brown) overlap with one another along LD1

Table 2. Genetic similarity matrix of Rhynchophorus spp. based on COI sequences. EBBM and EBMin show ~8–9% divergence, suggesting possible subspecies or distinct species status. EBMan, EBSTS, EBSTU, and EBTam exhibit 100% similarity, indicating a single species with no significant genetic variation

	EBBM (%)	EBMan (%)	EBMin (%)	EBSTS (%)	EBSTU (%)	EBTam (%)
EBBM						
EBMan	91.64					
EMin	99.24	91.19				
EBSTS	91.64	100	91.19			
EBSTU	91.64	100	91.19	100		
EBTam	91.64	100	91.19	100	100	

their shared geographic origin from mainland North Sulawesi. However, both share only 91.64% and 91.19% similarity, respectively, with the Sangihe cluster (EBMan, EBSTS, EBTU, EBTam) indicating moderate divergence. These findings suggest that EBBM and EBMin exhibit a relatively high genetic divergence of approximately 8-9%, placing them near the threshold between intra- and interspecific variation. This level of differentiation may indicate incipient speciation, particularly when considered alongside significant morphological differences such as in rostrum length and antennal structure as previously demonstrated in morphometric analyses.

In contrast, EBMan, EBSTS, EBTU, and EBTam exhibit 100% COI sequence similarity, confirming complete genetic identity among them. Their shared morphometric and genetic profiles suggest they constitute a single, genetically homogeneous taxon. These results indicate potential geographic structuring within *R. vulneratus*, with EBBM and EBMin possibly representing an emerging lineage isolated from the genetically uniform Sangihe cluster.

The phylogenetic tree (Figure 6) shows that all six EB specimens (EBBM, EBMin, EBMan, EBSTS, EBTam, and EBSTU) fall within the R. vulneratus clade, yet they separate into two well-supported subgroups. The EBBM and EBMin specimens, originating from Minahasa and Bolaang Mongondow Regencies on mainland North Sulawesi, form a distinct cluster with high bootstrap support, suggesting that they may represent a genetically unique lineage or geographically isolated populations. In contrast, the EBMan, EBSTS, EBTam, and EBSTU specimens collected from the Sangihe Islands regency group together in another clade with strong support (92.2%), indicating that these populations share similar genetic characteristics but are distinct from the EBBM and EBMin group. This division implies potential genetic divergence influenced by ecological or geographical factors.

The barcoding gap analysis for *Rhynchophorus* spp. demonstrates a distinct separation between genetic distances within species and those between different species (Figure 7). Intraspecific distances, ranging from approximately 0 to 0.0981, are tightly clustered with a prominent peak at the lower end, indicating minimal variation within species. In contrast, interspecific distances span from roughly 0.0981 to 0.2572, reflecting greater divergence among species. The absence of overlap between these distributions, with a transition point at about 0.0981, provides a robust basis for using genetic distance as a criterion for species delineation. Thus, a threshold of approximately 0.0981 can be confidently employed: individuals with genetic differences below this value are considered conspecific, while those with differences above it are likely from different species.

4. Discussion

The comprehensive analysis of palm weevil specimens using both morphometric and molecular approaches provides robust evidence of inter- and intraspecific diversity. Morphometric analyses including one-way ANOVA and MANOVA evealed highly significant differences in key traits such as rostrum length, scape length, and coxal distances, with p-values ranging from 10^{-180} to 10^{-103}. These extremely low p-values underscore that the observed morphological differences are not random but are strongly influenced by geographic and ecological factors (Ribeiro *et al.* 2014; Nasir *et al.* 2020). PCA showed that nearly all morphometric variability was captured by the first two components, while LDA maximized the separation among populations.

Among the groups, EBBM consistently exhibited larger and more distinctive morphological features, particularly in rostrum length and body size, compared to other groups, forming a clearly isolated cluster

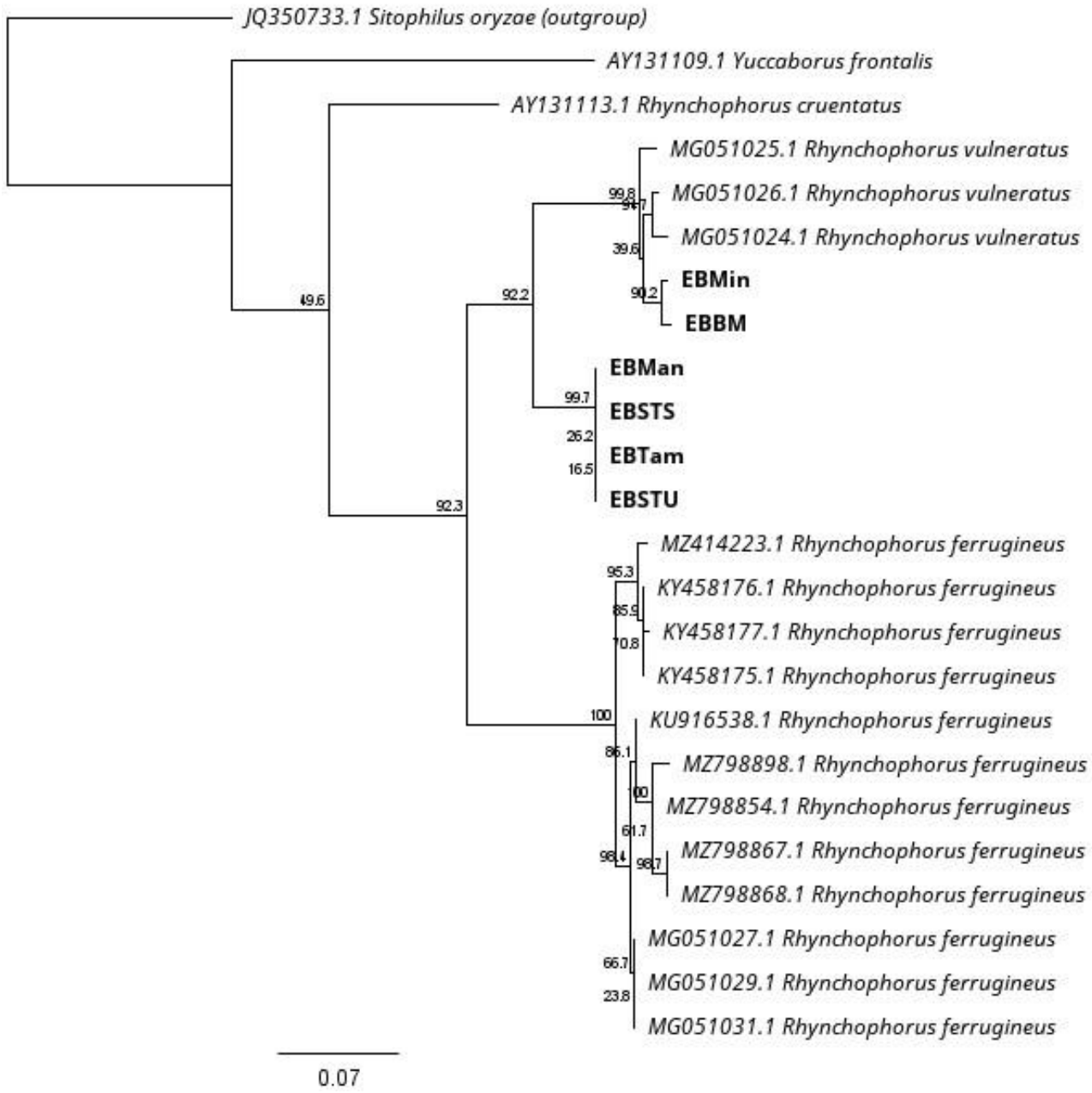

Figure 6. Phylogenetic tree showing the relationships among *Rhynchophorus* species, with EB specimens (EBBM, EBMin, EBMan, EBSTS, EBTam, and EBSTU) clustering within the *R. vulneratus* clade. EBBM and EBMin form a distinct subgroup with high bootstrap support (92.2%), while EBMan, EBSTS, EBTam, and EBSTU cluster together in another well-supported group (99.7%). The *R. vulneratus* clade, including the EB specimens, is clearly distinct from *R. ferrugineus* and *R. cruentatus*. Bootstrap values indicate strong support for the observed genetic relationships

in both PCA and LDA. These patterns suggest that localized adaptive divergence may be occurring, potentially driven by habitat fragmentation or resource specialization (Jacquemyn *et al.* 2012; Watanabe *et al.* 2014). This observation is corroborated by previous studies on Egyptian red palm weevils, which documented distinct variations in traits such as prothoracic spot patterns and specific body part measurements across different populations (El-Zoghby *et al.* 2022). These results suggest that local adaptation or genetic divergence could be responsible for the observed morphological differences, emphasizing the role of geographic and ecological influences on the evolution of these populations (Freudiger *et al.* 2021; White *et al.* 2022).

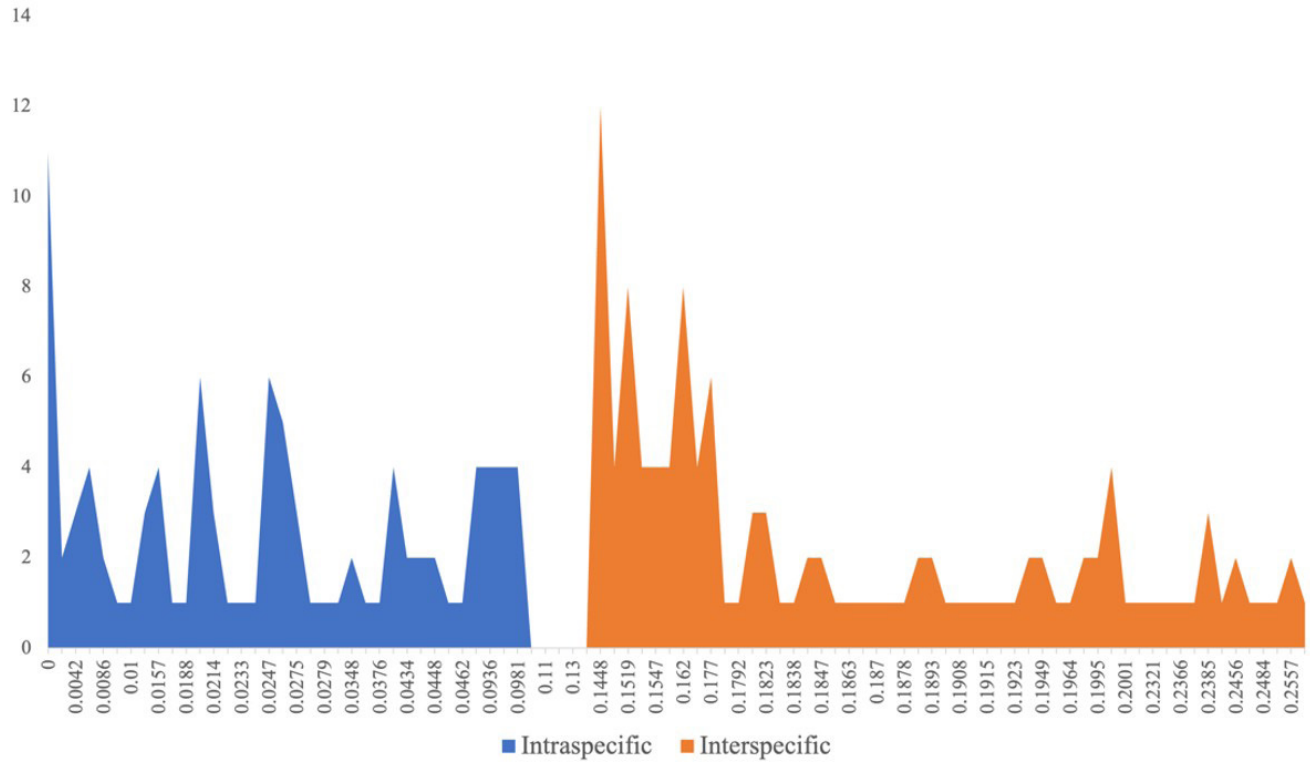

Figure 7. Barcoding gap analysis reveals distinct intraspecific (blue) and interspecific (orange) genetic distance distributions in *Rhynchophorus* spp. The clear separation, with lower intraspecific and higher interspecific distances, supports the effectiveness of COI as a marker for accurate species differentiation

Molecular evidence further supports the morphometric distinctions observed among populations. Phylogenetic analysis confirmed that all EB specimens belong to the *R. vulneratus* clade but are divided into two well-supported subgroups: EBBM and EBMin (mainland North Sulawesi), and EBMan, EBSTS, EBTam, and EBTU (Sangihe Islands). This phylogenetic structure mirrors the morphometric clustering and highlights the presence of geographically structured variation within *R. vulneratus*. The distinctiveness of EBBM and EBMin suggests genetic divergence driven by local adaptation or isolation (Hu *et al.* 2019), and their separation from the Sangihe cluster may represent an early stage of lineage differentiation.

These relationships were reinforced by maximum likelihood analysis with strong bootstrap support, which clearly distinguished the *R. vulneratus* clade from related species such as *R. ferrugineus* and *Sitophilus* spp. These findings strongly support classifying the red palm weevil color morphs-'ferrugineus' (orange with black markings) and 'vulneratus' (black with a red stripe)-as distinct species, as further validated by ITS1 and ITS2 barcode data (Sadder *et al.* 2015). The consistent clustering of EBMan, EBSTS, EBTam, and EBTU in both phylogenetic and morphometric analyses, despite being collected from different sites within Sangihe, indicates that these populations form a cohesive genetic unit. Their homogeneity may be maintained through gene flow or similar ecological pressures across the island group.

While phylogenetic substructure is evident particularly between the mainland and island populations all specimens were identified as *R. vulneratus*. Multiple lines of evidence support this classification. First, pairwise COI genetic distances remained below the conservative interspecific threshold of 9.81%, suggesting that the divergence observed remains within the bounds of intraspecific variation. Second, all sequences clustered consistently within the *R. vulneratus* clade, with no phylogenetic proximity to *R. ferrugineus* or *R. cruentatus*. Third, although morphometric and genetic divergence was detected, the degree of differentiation was insufficient-quantitatively or diagnostically-to justify species-level distinction under either biological or phylogenetic species concepts.

Genetic distance analysis revealed moderate divergence among groups, and barcode gap analysis showed a clear separation between intraspecific and interspecific variation. While the genetic divergence between EBBM/EBMin and the Sangihe populations remained below the 9.81% interspecific threshold, it was notably higher than typical within-group distances, suggesting potential population structuring or the onset of lineage differentiation. LDA results further support this interpretation, with EBBM forming a distinct cluster along both LD1 and LD2, while Sangihe groups showed partial overlap. These patterns align with the idea that local adaptation and restricted gene flow contribute to geographically influenced divergence within species (Lin *et al.* 2021; McGreevy *et al.* 2024). Interestingly, the observed genetic divergence among *R. vulneratus* specimens within the Sangihe Islands, despite their classification as the same species, suggests potential incipient population structuring or local adaptation within the island group. Such divergence, though not exceeding species-level thresholds, may reflect restricted gene flow, geographic isolation among islands, or ecological differentiation across microhabitats within the archipelago (Gorospe *et al.* 2025). These patterns are consistent with evolutionary processes such as allopatric divergence or founder effects, which are commonly observed in insular systems (Recuerda *et al.* 2024). Over time, if genetic differentiation continues to accumulate in response to isolation or selective pressures, these populations could diverge further, possibly leading to subspecies formation or cryptic speciation (Kalirad *et al.* 2024). Therefore, the genetic variability observed within the Sangihe *R. vulneratus* specimens has important implications for future taxonomic resolution, conservation prioritization, and pest management strategies that consider population-level differences.

A conservative threshold of approximately 9.81% genetic distance is deemed appropriate for delineating species boundaries in this group, as values above this mark signify a shift from intraspecific variation to interspecific divergence. In fact, a previous study demonstrated that a threshold of 9.18% effectively delimited more than 88% of Entiminae weevil species (Ma *et al.* 2022). Based on the present data, the integration of morphometric and molecular evidence supports the existence of at least two evolutionarily distinct population units within North Sulawesi, though they remain within species-level boundaries. This multidimensional approach provides more reliable species identification and reinforces the value of combining genetic and phenotypic data in taxonomic assessments.

These findings align with previous research highlighting the complex interplay between environmental factors and genetic divergence (Lee & Mitchell-Olds 2013). Recent studies emphasize that morphological traits and genetic markers often co-vary in response to local adaptation, driving evolutionary divergence and speciation (Freudiger *et al.* 2021; Wadgymar *et al.* 2022). By employing PCA, LDA, phylogenetic reconstruction, and barcode gap analysis, this study provides a comprehensive framework for understanding evolutionary differentiation in *R. vulneratus*. Collectively, the evidence supports the recognition of geographically structured population units in North Sulawesi, which has significant implications for taxonomy, conservation planning, and the development of location-specific pest management strategies.

In conclusion, this study revealed significant morphological and genetic divergence among palm weevil populations, driven by geographic and ecological factors. Combined analyses demonstrated pronounced, statistically significant differences in both morphometric and genetic parameters. Statistical analyses confirmed significant morphometric variation among populations. The three-dimensional PCA visualization distinctly isolated the EBBM population. Additionally, LDA clustered the populations into three groups, with EBBM separated, EBMan and EBTam overlapping, and the remaining populations also overlapping. These findings suggest that marked morphological divergence is influenced by geographic and ecological factors, which have significant implications for taxonomy, conservation, and management.

Phylogenetic analysis confirmed that all six EB specimens belong to the *R. vulneratus* clade, forming two well-supported subgroups. EBBM and EBMin, collected from mainland North Sulawesi, appear to represent a distinct genetic lineage, possibly reflecting geographic isolation. In contrast, EBMan, EBTS, EBTam, and EBTU from the Sangihe Islands share a common genetic background, clearly separated from the mainland group. Barcoding gap analysis further supported this distinction, revealing a sharp transition at 9.81% between intra- and interspecific genetic distances. This robust gap validates COI-based

genetic divergence as an effective criterion for species identification and delineation within *Rhynchophorus* spp.

References

Al-Saqer, S.M., 2012. A reliable identification system for red palm weevil. *American Journal of Applied Sciences*. 9, 1150–1157.

Alrefaei, A.F., Al-Mrshoud, M.F., Alotaibi, A.M., Ahmad, Z., Farooq, M., Albalawi, H.F., Albeshr, M.F., Alshehri, E., Almutairi, M.H., Pizzio, G.A., 2023. Molecular identification and phylogenetic analysis of cytochrome b gene from *Garra tibanica*, an endogenous species from Saudi Arabia. *Journal of King Saud University-Science*. 35, 102390. https://doi.org/https://doi.org/10.1016/j.jksus.2022.102390

Antonacci, R., Linguiti, G., Paradiso, F., Scalone, C., Fanizza, C., Ciani, E., Cipriano, G., Ciccarese, S., Carlucci, R., 2023. Mitochondrial DNA diversity and genetic structure of striped dolphin *Stenella coeruleoalba* in the Northern Ionian Sea. *Frontiers in Marine Science.* 10, 1-17. https://doi.org/10.3389/fmars.2023.1088598

Caraballo, D.A., Montani, M.E., Martínez, L.M., Antoniazzi, L.R., Sambrana, T.C., Fernández, C., Cisterna, D.M., Beltrán, F.J., Colombo, V.C., 2021. Heterogeneous taxonomic resolution of cytochrome b gene identification of bats from Argentina: implications for field studies. *PLoS One.* 15, e0244750. https://doi.org/10.1371/journal.pone.0244750

Edelaar, P., 2018. Ecological speciation: when and how variation among environments can drive population divergence, in: Tietze, D. (Eds.), *Bird Species*. *Fascinating Life Sciences.* Springer, Cham, pp. 195-215. https://doi.org/10.1007/978-3-319-91689-7_11

Ehara, H., Naito, H., Toyota, K., Asano, K., Mishima, T., Isono, N., Ohmi, M., Nitta, Y., Toyoda, Y., 2020. Sustainable production and utilization of sago palm resource. *IOP Conf. Ser.: Earth Environ. Sci.* 418, 012005.

El-Zoghby, I.R.M., Awad, N.S., Alkhaibari, A.M., Abdel-Hameid, N.F., 2022. Ultrastructure traits and genetic variability of red palm weevil *Rhynchophorus ferrugineus* (Olivier) adults from different geographical locations in Egypt. *Diversity*. 14, 404. https://doi.org/10.3390/d14050404

Folmer, O., Black, M., Hoeh, W., Lutz, R., Vrijenhoek, R., 1994. DNA primers for amplification of mitochondrial cytochrome c oxidase subunit I from diverse metazoan invertebrates. *Molecular Marine Biology and Biotechnology*. 3, 294-299.

Freudiger, A., Josi, D., Thünken, T., Herder, F., Flury, J.M., Marques, D.A., Taborsky, M., Frommen, J.G., 2021. Ecological variation drives morphological differentiation in a highly social vertebrate. *Functional Ecology*. 35, 2266-2281. https://doi.org/https://doi.org/10.1111/1365-2435.13857

Gorospe, J.M., Záveská, E., Chala, D., Gizaw, A., Tusiime, F.M., Gustafsson, A.L.S., Piálek, L., Kolář, F., Brochmann, C., Schmickl, R., 2025. Ecological speciation with gene flow followed initial large-scale geographic speciation in the enigmatic afroalpine giant senecios (Dendrosenecio). *New Phytologist*. 246, 2307-2323. https://doi.org/https://doi.org/10.1111/nph.20432

Guindon, S., Dufayard, J.F., Lefort, V., Anisimova, M., Hordijk, W., Gascuel, O., 2010. New algorithms and methods to estimate maximum-likelihood phylogenies: assessing the performance of PhyML 3.0. *Systematic Biology*. 59, 307–321. https://doi.org/10.1093/sysbio/syq010

Hastuty, S., 2016. Pengolahan ulat sagu (*Rhynchophorus ferrugineus*) di Kelurahan Bosso Kecamatan Walenrang Utara Kabupaten Luwu. *Jurnal Perspektif.* 1, 12-19.

Hu, C.C., Wu, Y.Q., Ma, L., Chen, Y.J., Ji, X., 2019. Genetic and morphological divergence among three closely related *Phrynocephalus* species (Agamidae). *BMC Evolutionary Biology*. 19, 114. https://doi.org/10.1186/s12862-019-1443-y

Jacquemyn, H., De Meester, L., Jongejans, E., Honnay, O., 2012. Evolutionary changes in plant reproductive traits following habitat fragmentation and their consequences for population fitness. *Journal of Ecology*. 100, 76-87. https://doi.org/10.1111/j.1365-2745.2011.01919.x

Kalirad, A., Burch, C.L., Azevedo, R.B.R., 2024. Genetic drift promotes and recombination hinders speciation on holey fitness landscapes. *PLoS Genetics.* 20, e1011126. https://doi.org/10.1371/journal.pgen.1011126

Kimura, M., 1980. A simple method for estimating evolutionary rates of base substitutions through comparative studies of nucleotide sequences. *Journal of Molecular Evolution*. 16, 111-120. https://doi.org/10.1007/BF01731581

Kolondam, B.J., Tallei, T.E., Koneri, R., Abas, A.H., Mamahit, J.M.E., 2023. A review on mitochondrial genome of ants (Hymenoptera: Formicidae). *Heca Journal of Applied Sciences*. 1, 48-53.

Korua, S., Pelealu, J., Tulung, M., Mandey, L., Semuel, M.K., 2016. Molecular barcoding and phylogeny reconstruction of *Rhynchoporus* sp. in Minahasa North Sulawesi based partial cytochrome oxidase subunit 1 gene (CO1). *Journal of Natural Sciences Research*. 6, 42-52.

Lee, C.R., Mitchell-Olds, T., 2013. Complex trait divergence contributes to environmental niche differentiation in ecological speciation of *Boechera stricta. Molecular Ecology*. 22, 2204-2217. https://doi.org/10.1111/mec.12250

Lin, Y.P., Mitchell-Olds, T., Lee, C.R., 2021. The ecological, genetic and genomic architecture of local adaptation and population differentiation in *Boechera stricta*. *Proceedings. Biological Sciences*. 288, 20202472. https://doi.org/10.1098/rspb.2020.2472

Lombogia, C.A., Posangi, J., Pollo, H.N., Tulung, M., Tallei, T.E., 2020. Assessment of genetic variation in *Apis nigrocincta* (Hymenoptera: Apidae) in Sulawesi revealed by partial mitochondrial cytochrome oxidase I gene sequences. *Scientifica*. 2020, 1609473. https://doi.org/10.1155/2020/1609473

Ma, Z., Ren, J., Zhang, R., 2022. Identifying the genetic distance threshold for Entiminae (Coleoptera: Curculionidae) species delimitation via COI Barcodes. *Insects*. 13, 261. https://doi.org/10.3390/insects13030261

McGreevy, T.J., Crawford, N.G., Legreneur, P., Schneider, C.J., 2024. Influence of geographic isolation and the environment on gene flow among phenotypically diverse lizards. *Heredity*. 133, 317-330. https://doi.org/10.1038/s41437-024-00716-y

Montagna, M., Chouaia, B., Mazza, G., Prosdocimi, E. M., Crotti, E., Mereghetti, V., Vacchini, V., Giorgi, A., De Biase, A., Longo, S., Cervo, R., Lozzia, G. C., Alma, A., Bandi, C., Daffonchio, D., 2015. Effects of the diet on the microbiota of the red palm weevil (Coleoptera: Dryophthoridae). *PloS One*. 10, e0117439. https://doi.org/10.1371/journal.pone.0117439

Nasir, D.M., Mamat, N.S., Muneim, N.A.A., Ong-Abdullah, M., Latip, N.A.A., Su, S., Hazmi, I.R., 2020. Morphometric analysis of the oil palm pollinating weevil, *Elaeidobius kamerunicus* (Faust, 1878) (Coleoptera: Curculionidae) from oil palm plantations in Malaysia. *Journal of the Entomological Research Society*. 22, 275-291. https://api.semanticscholar.org/CorpusID:229370112

Nishimaki, T., Sato, K., 2019. An extension of the Kimura two-parameter model to the natural evolutionary process. *Journal of Molecular Evolution*. 87, 60-67. https://doi.org/10.1007/s00239-018-9885-1

Nurlydia, B.S.S., Riza, B.H.I., Fatimah, B.A., Faszly, B.R., Aziz, J.A., 2019. Population variation of the red stripe weevils, *Rhynchophorus vulneratus* (Coleoptera: Curculionidae) isolated by geographical limit. *The Raffles Bulletin of Zoology*. 67, 378–384.

Direktorat Jenderal Perkebunan Kementerian Pertanian Republik Indonesia, 2020. Statistik Perkebunan Unggulan Nasional 2019-2021. Available at https://ditjenbun.pertanian.go.id/template/uploads/2021/04/BUKU-STATISTIK-PERKEBUNAN-2019-2021-OK.pdf. [Date accessed: 9 January 2025]

Phillips, J.D., Griswold, C.K., Young, R.G., Hubert, N., Hanner, R.H., 2024. A measure of the DNA barcode gap for applied and basic research. *Methods in Molecular Biology.* 2744, 375-390. https://doi.org/10.1007/978-1-0716-3581-0_24

Ramzan, R., Kadenbach, B., Vogt, S., 2021. Multiple mechanisms regulate eukaryotic cytochrome c oxidase. *Cells*. 10, 514. https://doi.org/10.3390/cells10030514

Recuerda, M., Montoya, J.C.H., Blanco, G., Milá, B., 2024. Repeated evolution on oceanic islands: comparative genomics reveals species-specific processes in birds. *BMC Ecology and Evolution*. 24, 140. https://doi.org/10.1186/s12862-024-02320-4

Ribeiro, Â.M., Lloyd, P., Dean, W.R.J., Brown, M., Bowie, R.C.K., 2014. The ecological and geographic context of morphological and genetic divergence in an understorey-dwelling bird. *PloS One*. 9, 1-11. https://doi.org/10.1371/journal.pone.0085903

Rochat, D., Dembilio, O., Jaques, J.A., Suma, P., Pergola, A., La, Hamidi, R., Kontodimas, D., Soroker, V., 2017. *Rhynchophorus ferrugineus*: taxonomy, distribution, biology, and life cycle. Handbook of Major Palm Pests. pp. 69-104. https://doi.org/10.1002/9781119057468.ch4

Rozziansha, T.A.P., Hidayat, P., Harahap, I.S., 2021. Morphological characters of *Rhynchophorus* spp. (Coleoptera:Curculionidae) associated with sago, coconut, and oil palm in Indonesia. *IOP Conf. Ser.: Earth Environ. Sci.* 694, 012051

Rugman-Jones, P.F., Hoddle, C.D., Hoddle, M.S., Stouthamer, R., 2013. The lesser of two weevils: molecular-genetics of pest palm weevil populations confirm *Rhynchophorus vulneratus* (Panzer 1798) as a valid species distinct from *R. ferrugineus* (Olivier 1790), and reveal the global extent of both. *PloS One*. 8, e78379. https://doi.org/10.1371/journal.pone.0078379

Sadder, M.T., Vidyasagar, P.S.P.V., Aldosari, S.A., Abdelazim, M.M., Al-Doss, A.A., 2015. Phylogeny of red palm weevil (*Rhynchophorus ferrugineus*) based on ITS1 and ITS2. *Oriental Insects*. 49, 198-211.

Satiman, U., Tulung, M., Pelealu, J., Salaki, C., Kolondam, B., Tallei, T., Emran, T., Pinaria, A., 2022. Morphology, diversity and phylogenetic analysis of *Spodoptera exigua* (Lepidoptera: Noctuidae) in North Sulawesi by employing partial mitochondrial cytochrome oxidase 1 gene sequences. *J Adv Biotechnol Exp Ther.* 5, 136-147. https://doi.org/10.5455/jabet.2022.d103

Seman-Kamarulzaman, A.F., Pariamiskal, F.A., Azidi, A.N., Hassan, M., 2023. A review on digestive system of *Rhynchophorus ferrugineus* as potential target to develop control strategies. *Insects.* 14, 506. https://doi.org/10.3390/insects14060506

Sholihah, A., Delrieu-Trottin, E., Sukmono, T., Dahruddin, H., Risdawati, R., Elvyra, R., Wibowo, A., Kustiati, K., Busson, F., Sauri, S., Nurhaman, U., Dounias, E., Zein, M.S.A., Fitriana, Y., Utama, I.V., Muchlisin, Z.A., Agnèse, J.F., Hanner, R., Wowor, D., … Hubert, N., 2020. Disentangling the taxonomy of the subfamily Rasborinae (Cypriniformes, Danionidae) in Sundaland using DNA barcodes. *Scientific Reports*. 10, 2818. https://doi.org/10.1038/s41598-020-59544-9

Stelbrink, B., Albrecht, C., Hall, R., von Rintelen, T., 2012. The biogeography of Sulawesi Revisited: is there evidence for a vicariant origin of taxa on Wallace's "Anomalous Island"? *Evolution*. 66, 2252–2271. https://doi.org/https://doi.org/10.1111/j.1558-5646.2012.01588.x

Stout, L., Daffe, G., Chambouvet, A., Correia, S., Culloty, S., Freitas, R., Iglesias, D., Jensen, K.T., Joaquim, S., Lynch, S., Magalhães, L., Mahony, K., Malham, S.K., Matias, D., Rocroy, M., Thieltges, D.W., de Montaudouin, X., 2024. Morphological vs. molecular identification of trematode species infecting the edible cockle *Cerastoderma edule* across Europe. *International Journal for Parasitology: Parasites and Wildlife*. 25, 1-13. https://doi.org/https://doi.org/10.1016/j.ijppaw.2024.101019

Sukirno, S., Tufail, M., Rasool, K.G., Aldawood, A.S., 2018. Description of phenotypic variability in Asiatic palm weevil, *Rhynchophorus vulneratus* (Coleoptera: Culculionidae). *Journal of the Entomological Research Society*. 20, 1-22.

Tallei, T., Koneri, R., Kolondam, B., 2017. Sequence analysis of the cytochrome c oxidase subunit I gene of *Pseudagrion pilidorsum* (Odonata: Coenagrionidae). *Makara Journal of Science*. 21, 43-52.

Tallei, T., Pelealu, J., Kolonam, B., Batiha, G., Lubis, L., Mahmud, S., Emran, T., 2021. A molecular phylogeny of Taeniophyllum THRJ inferred from DNA barcode regions. *Journal of Advanced Biotechnology and Experimental Therapeutics*. 4, 171-177. https://doi.org/10.5455/jabet.2021.d117

Wadgymar, S.M., DeMarche, M.L., Josephs, E.B., Sheth, S.N., Anderson, J.T., 2022. Local adaptation: causal agents of selection and adaptive trait divergence. *Annual Review of Ecology, Evolution, and Systematics*. 53, 87-111. https://doi.org/10.1146/annurev-ecolsys-012722-035231

Watanabe, K., Kazama, S., Omura, T., Monaghan, M.T., 2014. Adaptive genetic divergence along narrow environmental gradients in four stream insects. *PloS One*. 9, 1-9. https://doi.org/10.1371/journal.pone.0093055

White, N.J., Beckerman, A.P., Snook, R.R., Brockhurst, M.A., Butlin, R.K., Eyres, I., 2022. Experimental evolution of local adaptation under unidimensional and multidimensional selection. *Current Biology*. 32, 1310-1318.e4. https://doi.org/https://doi.org/10.1016/j.cub.2022.01.048

Yong, K.W., Bakar, A.A., Azmi, W.A., 2015. Fecundity, fertility and survival of red palm weevil (*Rhynchophorus ferrugineus*) larvae reared on sago palm. *Sains Malaysiana*. 44, 1371–1375.